Identifying Patients with Epilepsy Having Depression/Anxiety Disorder using Common Spatial Patterns of Functional EEG Networks

Yuanyuan Zhang
College of Medicine, Southwest Jiaotong University, Chengdu
Kejun Du
College of Medicine, Southwest Jiaotong University, Chengdu
Zhichuang Qu
Southwest Medical University, Luzhou
Yuhang Lin
School of Life Science and Technology, University of Electronic Science and Technology of China, Chengdu,
Daqing Guo
School of Life Science and Technology, University of Electronic Science and Technology of China, Chengdu,
Xin Chen
Department of Neurosurgery, The General Hospital of Western Theater Command, Chengdu
Haifeng Shu
Department of Neurosurgery, The General Hospital of Western Theater Command, Chengdu
Sixun Yu (bingyutian1982@126.com)
Department of Neurosurgery, The General Hospital of Western Theater Command, Chengdu

Research Article

Keywords: Machine learning, Epilepsy with depression/anxiety disorder, spatial patterns of network (SPN)

Posted Date: April 7th, 2022

DOI: https://doi.org/10.21203/rs.3.rs-1512438/v1

Abstract

Background

The presentation of epilepsy with depression/anxiety disorder (E-AD) is a complex comorbidity, and a systematic psychiatric screen poses a heavy economic burden for the patients. Traditionally, distinguishing between E-AD patients and epilepsy without depression/anxiety disorder (E-no-AD) needs multiple evaluations, which is incredibly difficult owing to the high costs. Therefore, there is an urgent need for a reliable assessment protocol to initially distinguish between the two types of patients.

Results

Based on the resting-state electroencephalography signals collected from E-AD and E-no-AD patients, the classification performances were estimated for three different network features, using the support vector machine. The results revealed that the SPN feature of functional network connectivity was remarkably superior to the traditional network feature for distinguishing between the two groups of patients, with appreciable classification accuracy values of 89.90% and 87.37% sensitivity and 91.67% specificity.

Conclusions

These findings demonstrate the superiority of functional SPN features as a reliable way in characterizing the differences of E-AD and E-no-AD patients and potentially provide insights for the complex mechanisms causing E-AD in patients.

Introduction

Epilepsy affects more than 70 million people globally, making it among the most common serious neurological disorders, and notably, active epilepsy in more than 75% of cases goes untreated, which represents a significant treatment gap, particularly in low-income and middle-income countries [1, 2]. Depression and anxiety are social dysfunction diseases primarily manifested by low mood. A survey showed that patients with epilepsy had a predisposition to develop some mood disorders, with depression and anxiety being the most common comorbidities of epilepsy [3]. The morbidity and mortality were higher for epilepsy patients with depression/anxiety disorders (E-AD) than for those without depression/anxiety disorders (E-no-AD)[4, 5]. Owing to the close relationship between epilepsy and depression/anxiety, both individuals and the society stand to greatly benefit from an effective method for diagnosing epilepsy comorbid depression [6–8]. The existing diagnosis are mainly based on the assessment of patient scales, and the long-term evaluation process will bring huge economic burdens for patients. On the other hand, the scale-based methods are greatly affected by the patients' state and the physicians' experience, making assessment very unstable.

Electroencephalography (EEG) is easily accessible and relatively inexpensive [9], which has led to its widespread use for the diagnosis and classification of epilepsy and mental disorders. The characteristic of EEG signals allows us to distinguish specific pattern, including the identification of patients with epilepsy [10, 11], the detection of epileptogenic focus localization [12, 13], and the prediction of depression and anxiety [14–16]. In theory, internal interactions among brain regions can be characterized using a functional network constructed from EEG signals; this would allow us to distinguish resting-state signals by differentiating specific network patterns [17–19]. In a clinical setting, EEG records can help estimate the degree and decide the optimal treatment of different diseases, which can help reduce the economic pressure [11, 20].

In previous studies, the complex networks or potential pathological abnormalities were described by graph theory [21, 22]. It is a reflection of a network and is represented by its connections and nodes. Several network properties can be used to describe the graphs, such as clustering coefficient, characteristic path length, local efficiency, and global efficiency. Overall connectedness is indicated by the characteristic path length, and the local connectedness of the graph is measured by the clustering coefficient [23–25]. However, the complete body of information within a network cannot be reflected in the properties represented by statistical measurements. This approach aims to use changes in connectedness to our advantage for classifying and identifying the anxiety state using EEG signals. Accordingly, not always can ideal performance be achieved by differentiation of specific brain networks on the basis of graph theory analysis findings. To this end, some classic EEG feature extraction methods have been proposed by researchers, such as the adaptive auto regressive model [26], wavelet transform [27, 28], empirical mode decomposition [29, 30], and the analysis of common spatial [31, 32]. Currently, the analysis of spatial pattern of network (SPN) is acknowledged as effective methods to reflect spatial features in an EEG network. The spatial information remarkably affects two-class EEG signal classification; in a training data set, this algorithm computes spatial filters that minimize the variance of one class and maximize the variance of the other [33, 34]. The superiority of such spatial information has been confirmed in previous related studies for several purposes, such as predicting epilepsy seizures [35, 36], differentiating between patients with schizophrenia vs. healthy controls, and differentiating between psychogenic non-epileptic seizures vs. epileptic seizures [10, 37].

As we mentioned above, a stable, clinically usable method for distinguishing between E-AD and E-no-AD patients can help doctors with early detection, timely treatment, and non-invasive screening. However, it remains a challenge to directly differentiate the two groups of patients in the resting brain state. As both E-AD and E-no-AD are associated with brain network abnormalities [38–40], identifying inherent properties of the resting state network may help distinguish between the two groups. Herein, the resting-state EEG signals were collected from 11 E-no-AD patients and 15 E-AD patients and were used to construct functional networks. We attempted to realize a stable differentiation of E-AD patients and E-no-AD patients based on the spatial features of functional networks. For the comparison of the classification performance, we also estimated the accuracy of the classification based on the traditional network

properties and the classic principal component analysis from the functional networks. According to our final results, the SPN feature of functional network connectivity showed great superiority to the traditional network features for distinguishing between E-AD patients and E-no-AD patients.

Results

In this study, we built functional networks in different frequency bands, and the classification performance was evaluated on the basis of network features, which included network properties, SPN features, and principal components of networks. First, we compared the network properties of the functional networks in different frequency bands for E-no-AD and E-AD patient groups. As shown in Fig. 2, we found the four network properties, namely characteristic path length, clustering coefficient, local efficiency, and global efficiency, to exhibit no between-group differences, thus making it challenging to differentiate between the two patient groups only on the basis of network properties (as shown in Table I). For comparison purposes, we also performed the classification on the basis of principal components and spatial features of networks. For most frequency bands, the principal components of functional networks were superior to the network properties in differentiating between E-no-AD patients and E-AD patients. However, principal component analysis (PCA) did not achieve ideal classification performance, and the best accuracy rate obtained was 66.31%. Therefore, the two abovementioned methods may not be suitable for the actual clinical diagnosis. Instead, the SPN features realized stable classification for E-no-AD and E-AD patients in different frequency bands. Considering the potential redundancy as well as the classification performance, we herein chose four pairs of spatial filters for SPN feature extraction. Further, we found that the SPN features in beta bands had the highest recognition rate with an accuracy of 89.90%.

To further explore the potential differences in functional networks between the patient groups, we checked for significant differences in the connectivity strength ($p < 0.01$) of functional networks in different frequency bands. The connectivity strength did not statistically significantly differ in most frequency bands (Fig. 3). However, in some particular frequency bands, abnormal connectivity strength was occasionally observed. To be specific, the connectivity strength between the frontal lobe and the parietal lobe was significantly decreased in E-AD patients when compared with E-no-AD patients in the beta-band functional network, which may have translated into the better classification performance of the beta-band SPN features. In addition, the brain regions recorded by the electrodes P4 and Fp1 were of great significance in distinguishing between the two patient groups. Conversely, similar statistical differences were noted along with the full frequency band as well; however, the trend overall was weakened by the influence of other frequency bands.

The first pair SPN filters obtained from the functional networks in the beta band is shown in Fig. 4; it was found to exhibit the best classification performance. In theory, the SPN features extracted by the first SPN filter have the most discriminative potential for the two patient groups. Notably, the comparisons of both connectivity strengths and SPN filters (Fig. 3 and Fig. 4) potentially reflect differences in functional networks. Figure 3 shows statistical differences among all brain regions, while Fig. 4 emphasizes the

discriminative properties of some crucial nodes extracted by the first pair of SPN filters. Furthermore, it should be noted that several non-statistical features underrepresented by statistical comparison may also have influenced the SPN filters. These factors indicated that even though both statistical comparison and SPN filters exhibited differences in the connectivity strength for E-AD and E-no-AD patients, the two results are not completely identical.

Discussion

Previous studies have described the human brain as a large-scale network having multiple brain regions that interact with one another to process complex and changing information. Therefore, when the brain region becomes the epileptic focus, other functions, such as epilepsy-related anxiety/depression, are bound to be affected. In this study, we used resting scalp EEG signals and achieved stable classification of two types of epilepsy patients (E-no-AD patients and E-AD patients). By distinguishing among patients on the basis of the spatial features extracted by SPN filters, we differentiated between E-AD and E-no-AD patients with 89.90% accuracy. We further confirmed our conclusion in two ways: SPN features of functional networks could help distinguish between the two patient types with high accuracy, whereas the traditional network properties and principal component were not as effective in making this distinction.

Considering the possibility that the cognitive deficits incurred by the depression/anxiety disorder may be reflected in the brain regions related to these disorders, we attempted the use of network properties to assess and compare brain efficiency between E-AD and E-no-AD patients [52, 53]. However, this classification achieved unsatisfactory accuracy in distinguishing the two patient types. Theoretically, the network properties are directly statistical measurements and cannot contain the complete information of network differences. The results shown in Fig. 2 also prove that the resting-state functional network properties were not significantly different. Conversely, to present the spatial topography of the abnormal components and extract abnormal components from EEG signals, PCA could be an effective method [54]. As shown in Table I, the classification based on PCA components showed evidently better performance than that based on network properties. However, such differentiation did not meet the requirements for practical use.

In previous studies, the superiority of the spatial topology information in recognizing the abnormal networks has been established [55]. The analysis of spatial patterns is an effective way to extract the spatial features of networks. In theory, SPN filters can reflect critical nodes that exhibit significantly different connectivity strengths in the networks by endowing relatively larger weights. In the present study, appropriate SPN filters revealed a discriminative feature between E-AD and E-no-AD patients. As shown in Fig. 4, the brain regions exhibiting significant differences in the statistical comparison were emphasized with larger coefficients while the others were compressed with smaller coefficients. Accordingly, we achieved a reliable classification performance on the basis of such spatial features extracted by the spatial filters.

We compared the classification performance of the SPN features in different frequency bands and found that the functional networks in the beta band could be crucial in distinguishing between E-AD and E-no-AD patients. It has been previously reported that the beta-band activity in resting-state is closely related to the development of neurological diseases [56, 57]. Further, on the basis of the statistical comparison of the beta-band functional network shown in Fig. 3, we found the critical brain regions that may be closely related to the pathological differences between the two patient types. For instance, we found that the connectivity between frontal and parietal lobes was significantly weaker in E-AD patients than in E-no-AD patients, which could help distinguish between the two types of patients. In addition, a close relation between these brain regions and the depression/anxiety disorder has also been suggested [58].

Conclusion

Within the scope of this article, we propose that spatial features of functional networks can be applied to differentiate between E-no-AD and E-AD patients. Notably, our approach was based on the resting-state scalp EEG and did not require long-term clinical observation; this could greatly reduce the economic pressure of patients. However, this study has some limitations. First, the dataset used here is relatively small and needs further expansion for subsequent studies. Second, although the classification based on the SPN features of functional networks performed well in this study, its suitability to other neurological diseases needs to be determined. Besides, we herein did not implement several alternative methods to estimate the brain networks, such as Granger causality or transfer entropy for effective networks and multiple autoregressive models for functional network [59–61]. In future studies, a classification based on fused features of both effective and functional networks deserves an attempt for a higher accuracy rate as it may offer better discriminating abilities owing to the advantages of a high-dimensional feature space.

Methods

A. EEG dataset

We collected the resting-state EEG signals of patients with epilepsy from the General Hospital of Western Theater Command PLA. The EEG was performed with locations according to the international 10-20 system using 21 Ag-AgCl electrodes. Next, we sampled all signals at 500 Hz with a 50-Hz notch filter and a 0.01–100-Hz bandpass filter. The Ethics Committee of The General Hospital of Western Theater Command PLA approved all experimental protocols. All participants provided written informed consent, and the study was performed in compliance with the tenets of the Declaration of Helsinki. Two senior epileptologists having extensive experience in diagnosis and treatment of epilepsy established the diagnosis.

After careful review, patients to be included for analyses were selected by two senior epileptologists with extensive experience in diagnosis and treatment of epilepsy. They selected 15 E-AD patients (age, 18–57 years) and 11 E-no-AD patients (age, 19–46 years). The following were the inclusion criteria for the

screened E-AD patients: 1) Each patient underwent an outpatient or inpatient video-EEG recording for ≤24 h, two senior experts confirmed that the segments were recorded during the resting state, 2) A confirmed diagnosis of epilepsy was established by two senior experts, 3) Both groups of patients were assessed using the Hamilton Mood Scale or Self-Rating Anxiety/Depression Scale (SAS/SDS) by professional physicians [41, 42] and were identified as having anxiety/depression disorder, and 4) the treatment did not involve the use of any mood-altering drugs [43]. The E-no-AD patients included herein were screened using all the same standards except for not being detected as having anxiety/depression disorder. First, using the reference electrode standardization technique, the data were transformed to the approximate zero reference for reducing the impact of the reference effect [44]. Continuous EEG data were randomly divided into five-second segments for each patient, and high-amplitude segments (>100 μV) were excluded. Finally, 6346 and 4416 EEG segments for E-AD and E-no-AD patients were selected for the next step, respectively.

B. Functional networks

Herein, based on the resting-state EEG signals of different epilepsy patients, the functional networks were estimated. We considered six well-known frequency bands, which included the full frequency band (0.1–100 Hz), the delta band (0.1–4 Hz), the gamma band (30–100 Hz), the alpha band (8–13 Hz), the beta band (13–30 Hz), and the theta band (4–8 Hz) [45].

Coherence (Coh) was used to measure the connection strength between each pair of electrodes for establishing the functional network. In theory, for analyzing the cooperative, synchrony-defined cortical neuronal assemblies, Coh is the most commonly used metric. This metric represents a linear relationship at a specific frequency between two signals [$x(t)$ and $y(t)$] on the basis of their cross-spectrum. Notably, to indicate the linkage strength between two network nodes, we herein adopted frequency-specific coherence. Coh was expressed using the following formula [46]:

$$Coh(f) = \frac{P_{xy}(f)^2}{P_{xx}(f)P_{yy}(f)}$$

where $P_{xy}(f)$ is the cross-spectrum between $x(t)$ and $y(t)$, and $P_{xx}(f)$ and $P_{yy}(f)$ are the respective auto-spectra at frequency f estimated from the Welch-based spectrum at 0.1-Hz resolution. For each frequency band, the coherence matrices of all frequency points in this band were averaged to compute the coherence matrix.

C. Network Properties

For measuring the network topology property, we herein used several network measurements, such as global and local efficiency, characteristic path length, and clustering coefficient. We calculated the

clustering coefficient (CC) as follows [47]:

$$CC = \frac{1}{N}\sum_{i\in N}\frac{\sum_{j,h\in N}\left(\omega_{ij}\omega_{ih}\omega_{jh}\right)^{\frac{1}{3}}}{k_i k_{i-1}}$$

wherein k_i is the degree of node i, and ω_{ij} is the weight between nodes i and j in the network. A network's characteristic path length (L) when L_{ij} is the shortest path length between two nodes was calculated as follows:

$$L = \frac{1}{N}\sum_{i\in N}\frac{\sum_{j\in N, i\neq j} d_{ij}}{N-1}$$

The global efficiency (E_g) was computed using the following formula [48]:

$$E_g = \frac{1}{N}\sum_{i\in N}\frac{\sum_{j\in N, i\neq j} {d_{ij}}^{-1}}{N-1}$$

The local efficiency (E_i) of node i was defined as follows:

$$E_i = \frac{1}{2}\sum_{i\in N}\frac{\sum_{j,h\in N, i\neq j}\left(\omega_{ij}\omega_{ih}\left[d_{jh}\left(N_i\right)^{-1}\right]\right)^{\frac{1}{3}}}{k_i k_{i-1}}$$

We used the Brain Connectivity Toolbox (http://www.brain-connectivity-toolbox.net/, Rubinov et. al) to calculate the above network properties. The authors have reported on more detailed descriptions of the network topology properties [48].

D. Principal Component Analysis

Principal component analysis (PCA) was aimed to transform a number of correlated variables into a significant smaller number of uncorrelated variables, called principal components. It has a wide range of applications, such as de-noising signals, cluster analysis, feature reduction, and pattern recognition.

Let the centered data input vectors be $x_t (t = 1, ..., land \sum x_t = 0)$, each of which is of m dimension defined by $x_t = [x_t(1), x_t(2), ..., x_t(m)]^T$ (usually $m < l$), and s_t linearly transforms each vector x_t as:

$$s_t = U^T \bullet x_{t,}$$

The eigenvalue of the principal components could be calculated as follows:

$$\lambda_i u_i = C \bullet u_{i,}$$

where λ_i is the eigenvalue of C. Then, the principal components of s_i could be computed as follows:

$$s_t(i) = u_i^T x_t.$$

E. Spatial Patterns Networks

For distinguishing between normal and abnormal EEG or EEG components, the use of common spatial pattern (CSP) analysis was proposed in the early 1990s [33, 34]. SPN is primarily aimed at identifying the CSPs among various weighted brain network topologies. Therefore, as is the case with canonical CSP, the SPN-extracted spatial pattern is not in the physical data space but rather in the network space [49].

Let ϕ_1 and ϕ_2 be the $N \times N$ centered matrices for each subject; the spatial filters are the projections that maximize the following function [10, 34]:

$$J(\omega) = \frac{\omega^T \phi_1^T \phi_1 \omega}{\omega^T \phi_2^T \phi_2 \omega} = \frac{\omega^T \Phi_1 \omega}{\omega^T \Phi_2 \omega}$$

Here Φ_1 and Φ_2 are the covariance matrices of the adjacency matrix for the two groups. The objective function can be written as follows upon the introduction of the Lagrange multiplier:

$$L(\omega, \lambda) = \omega^T \Phi_1 \omega - \lambda(\omega^T \Phi_2 \omega - 1)$$

Under the condition $\frac{\partial L}{\partial \lambda} = 0$, the generalized eigenvalue equation can be used to estimate the objective projection ω.

$$\Phi_2^{-1} \Phi_1 W = \sum W$$

where W is the matrix comprising eigenvectors of $\Phi_2^{-1} \Phi_1$ and $\sum = diag(\lambda_1, \lambda_2, \ldots \lambda_m)$ with λ variables representing corresponding singular values [49].

F. Pattern Recognition

Herein, to realize the distinguishing of E-AD patients and E-no-AD patients, we performed the analysis and the feature extraction in the collected EEG datasets. As schematically shown in Fig. 1, we constructed the functional networks from the resting-state EEG segments. Then, for evaluating the classification performance, four traditional network properties (characteristic path length, clustering coefficient, local efficiency, and global efficiency), the PCA features of the network, and SPN features of the network were extracted. Then, we compared the classification performances to identify effective features for distinguishing between E-no-AD and E-AD patients. Notably, to explore the mechanism, the above comparisons were repeated in different frequency bands. For each feature, we introduced a support vector machine (SVM) classifier to learn feature distribution [50]. Next, to determine the optimized set of

parameters, we implemented a grid search approach. It was ensured that the process for each step in the testing set was the same as that in the training set [51]. To ensure reproducibility of results, 5-fold cross-validation was used to evaluate prediction results for validation.

G. Statistical Testing

Herein, we employed two-sample Student's t-test for the comparisons of the connectivity strengths represented by the trial-averaged networks, where $p < 0.01$ was the threshold for significance. We also used it to assess the significant differences of network properties for E-AD patients and E-no-AD patients.

To evaluate the classification performance based on different features, the 5-fold cross-validation strategy was used for the testing process. In each evaluation, specifically, four-fifth of the segments in this dataset were used for training and the other segments were used for testing. Such process was repeated to ensure that all segments served as testing dataset. We herein used three evaluation metrics including specificity (SPE), sensitivity (SEN), accuracy (ACC) to make the assessment of the specific classification performance. Sensitivity and specificity values indicate missed diagnosis and misdiagnosis rates of E-AD patients, respectively; the preference is to keep these rates low, which indicates an overall better performance. Accuracy represents the probability of correct identification in all cases.

$$ACC = \frac{n + n_{NAD}}{N_{AD} + N_{NAD}} \times 100\%$$

$$SEN = \frac{n_{AD}}{N_{AD}} \times 100\%$$

$$SPE = \frac{n_{NAD}}{N_{NAD}} \times 100\%$$

where N_{AD} and N_{NAD} represent the total number of E-AD and E-no-AD patients, and n_{AD} and n_{NAD} represent the number of correctly identified EEG signals of these patients, respectively.

Declarations

Availability of data and materials

The datasets used and or analyzed during the current study are available from the corresponding authors on reasonable request.

Acknowledgments

We would like to thank Prof. Daqing Guo for insightful advice, and gratefully acknowledge Yuhang Lin and the co-workers of the Southwest Jiaotong University for the assistance in this work.

Funding

This work was supported in part by the Department of Science and Technology of Sichuan Province (Grant Number 2019YJ0274), the project of hospital management of the General Hospital of the Western Theater Command (Grant Number 2021-XZYG-B22), Joint research project (Grant Number 2019LH01), Military Medical Innovation Engineering Special (Grant Number 21WQ040) and Science and Technology Innovation Talent Project of Sichuan Provincial Department of Science and Technology (Grant Number 2022JDRC0041).

Conflict of interest

The authors declare that they have no conflict of interest.

Author Contributions

ZYY performed most of the data analysis and wrote the manuscript, QZC provided investigative assistance, LYH contributed to interpretation of the data and analyses. All of the authors have read and approved the manuscript.

Ethics approval

The Ethics Committee of The General Hospital of Western Theater Command PLA approved all experimental protocols. All participants provided written informed consent, and the study was performed in compliance with the tenets of the Declaration of Helsinki.

Consent to participate

Not applicable

References

1. Thijs, R.D., Surges, R., O'Brien, T.J., et al., Epilepsy in adults. Lancet, 2019. 393(10172): p. 689-701.
2. Saxena, S. and Li, S., Defeating epilepsy: A global public health commitment. Epilepsia open, 2017. 2(2): p. 153-155.
3. Keezer, M.R., Sisodiya, S.M. and Sander, J.W., Comorbidities of epilepsy: current concepts and future perspectives. Lancet Neurology, 2016. 15(1): p. 106-115.
4. Forsgren, L., PREVALENCE OF EPILEPSY IN ADULTS IN NORTHERN SWEDEN. Epilepsia, 1992. 33(3): p. 450-458.
5. Strine, T.W., Kobau, R., Chapman, D.P., et al., Psychological distress, comorbidities, and health Behaviors among US adults with seizures: Results from the 2002 National Health Interview Survey. Epilepsia, 2005. 46(7): p. 1133-1139.

6. Mendez, M.F., Cummings, J.L. and Benson, D.F., Depression in epilepsy. Significance and phenomenology. Archives of neurology, 1986. 43(8): p. 766-770.
7. Wisnousky, H., Lazzara, N., Ciarletta, M., et al., Rates and risk factors for suicidal ideation, suicide attempts and suicide deaths in persons with HIV: a protocol for a systematic review and meta-analysis. Bmj Open, 2021. 11(2).
8. Gaitatzis, A., Sisodiya, S.M. and Sander, J.W., The somatic comorbidity of epilepsy: A weighty but often unrecognized burden. Epilepsia, 2012. 53(8): p. 1282-1293.
9. Fisher, R.S., Boas, W.V., Blume, W., et al., Epileptic seizures and epilepsy: Definitions proposed by the International League against Epilepsy (ILAE) and the International Bureau for Epilepsy (IBE). Epilepsia, 2005. 46(4): p. 470-472.
10. Xu, P., Xiong, X., Xue, Q., et al., Differentiating Between Psychogenic Nonepileptic Seizures and Epilepsy Based on Common Spatial Pattern of Weighted EEG Resting Networks. Ieee Transactions on Biomedical Engineering, 2014. 61(6): p. 1747-1755.
11. Lin, Y., Du, P., Sun, H., et al., Identifying Refractory Epilepsy Without Structural Abnormalities by Fusing the Common Spatial Patterns of Functional and Effective EEG Networks. Ieee Transactions on Neural Systems and Rehabilitation Engineering, 2021. 29: p. 708-717.
12. Adkinson, J.A., Karumuri, B., Hutson, T.N., et al., Connectivity and Centrality Characteristics of the Epileptogenic Focus Using Directed Network Analysis. Ieee Transactions on Neural Systems and Rehabilitation Engineering, 2019. 27(1): p. 22-30.
13. Gavaret, M., Trebuchon, A., Bartolomei, F., et al., Source localization of scalp-EEG interictal spikes in posterior cortex epilepsies investigated by HR-EEG and SEEG. Epilepsia, 2009. 50(2): p. 276-289.
14. Shim, M., Jin, M.J., Im, C.-H., et al., Machine-learning-based classification between post-traumatic stress disorder and major depressive disorder using P300 features. Neuroimage-Clinical, 2019. 24.
15. Hasanzadeh, F., Mohebbi, M. and Rostami, R., Prediction of rTMS treatment response in major depressive disorder using machine learning techniques and nonlinear features of EEG signal. Journal of Affective Disorders, 2019. 256: p. 132-142.
16. Zandvakili, A., Philip, N.S., Jones, S.R., et al., Use of machine learning in predicting clinical response to transcranial magnetic stimulation in comorbid posttraumatic stress disorder and major depression: A resting state electroencephalography study. Journal of Affective Disorders, 2019. 252: p. 47-54.
17. Harper, Z.J., Welzig, C.M. and Ieee. Exploring Spatiotemporal Functional Connectivity Dynamics of the Human Brain using Convolutional and Recursive Neural Networks. in International Joint Conference on Neural Networks (IJCNN). 2019. Budapest, HUNGARY.
18. Sargolzaei, S., Cabrerizo, M., Goryawala, M., et al. Functional Connectivity Network based on Graph Analysis of Scalp EEG for Epileptic Classification. in IEEE Signal Processing in Medicine and Biology Symposium (SPMB). 2013. Brooklyn, NY.
19. Ramkiran, S., Sharma, A. and Rao, N.P., Resting-state anticorrelated networks in Schizophrenia. Psychiatry Research-Neuroimaging, 2019. 284: p. 1-8.

20. Farzan, F., Vernet, M., Shafi, M.M.D., et al., Characterizing and Modulating Brain Circuitry through Transcranial Magnetic Stimulation Combined with Electroencephalography. Frontiers in Neural Circuits, 2016. 10.
21. Afshari, S. and Jalili, M., Directed Functional Networks in Alzheimer's Disease: Disruption of Global and Local Connectivity Measures. Ieee Journal of Biomedical and Health Informatics, 2017. 21(4): p. 949-955.
22. Chiang, S. and Haneef, Z., Graph theory findings in the pathophysiology of temporal lobe epilepsy. Clinical Neurophysiology, 2014. 125(7): p. 1295-1305.
23. Stam, C.J., van der Made, Y., Pijnenburg, Y.A.L., et al., EEG synchronization in mild cognitive impairment and Alzheimer's disease. Acta Neurologica Scandinavica, 2003. 108(2): p. 90-96.
24. Stam, C.J., de Haan, W., Daffertshofer, A., et al., Graph theoretical analysis of magnetoencephalographic functional connectivity in Alzheimers disease. Brain, 2009. 132: p. 213-224.
25. Fox, M.D. and Raichle, M.E., Spontaneous fluctuations in brain activity observed with functional magnetic resonance imaging. Nature Reviews Neuroscience, 2007. 8(9): p. 700-711.
26. Muthuswamy, J. and Thakor, N.V., Spectral analysis methods for neurological signals. Journal of Neuroscience Methods, 1998. 83(1): p. 1-14.
27. Xie, T., Pei, J., Jia, C., et al., Comparison of digital filter and wavelet transform for extracting electroencephalogram rhythm. Sheng wu yi xue gong cheng xue za zhi = Journal of biomedical engineering = Shengwu yixue gongchengxue zazhi, 2009. 26(4): p. 743-7.
28. Zhang, Z., Kawabata, H. and Liu, Z.Q., Electroencephalogram analysis using fast wavelet transform. Computers in Biology and Medicine, 2001. 31(6): p. 429-440.
29. Runnov, A.E., Grubov, V.V., Khramova, M.V., et al. Dealing with noise and physiological artifacts in human EEG recordings: empirical mode methods. in Saratov Fall Meeting (SFM) / 4th International Symposium on Optics and Biophotonics - Laser Physics and Photonics XVII, and Computational Biophysics and Analysis of Biomedical Data III. 2016. Saratov, RUSSIA.
30. Zahra, A., Kanwal, N., Rehman, N.u., et al., Seizure detection from EEG signals using Multivariate Empirical Mode Decomposition. Computers in Biology and Medicine, 2017. 88: p. 132-141.
31. Miao, M., Hu, W., Yin, H., et al., Spatial-Frequency Feature Learning and Classification of Motor Imagery EEG Based on Deep Convolution Neural Network. Computational and Mathematical Methods in Medicine, 2020.
32. Sun, Z., Li, B., Duan, F., et al., WLnet: Towards an Approach for Robust Workload Estimation Based on Shallow Neural Networks. Ieee Access, 2021. 9: p. 3165-3173.
33. Koles, Z.J., Lind, J.C. and Florhenry, P., SPATIAL PATTERNS IN THE BACKGROUND EEG UNDERLYING MENTAL DISEASE IN MAN. Electroencephalography and Clinical Neurophysiology, 1994. 91(5): p. 319-328.
34. Koles, Z.J., Lazar, M.S. and Zhou, S.Z., Spatial patterns underlying population differences in the background EEG. Brain topography, 1990. 2(4): p. 275-284.

35. Wendling, F., Bartolomei, F. and Senhadji, L., Spatial analysis of intracerebral electroencephalographic signals in the time and frequency domain: identification of epileptogenic networks in partial epilepsy. Philosophical Transactions of the Royal Society a-Mathematical Physical and Engineering Sciences, 2009. 367(1887): p. 297-316.
36. Zhang, Y., Guo, Y., Yang, P., et al., Epilepsy Seizure Prediction on EEG Using Common Spatial Pattern and Convolutional Neural Network. Ieee Journal of Biomedical and Health Informatics, 2020. 24(2): p. 465-474.
37. Li, F., Wang, J., Liao, Y., et al., Differentiation of Schizophrenia by Combining the Spatial EEG Brain Network Patterns of Rest and Task P300. Ieee Transactions on Neural Systems and Rehabilitation Engineering, 2019. 27(4): p. 594-602.
38. Kim, M.-K., Kim, M., Oh, E., et al., A Review on the Computational Methods for Emotional State Estimation from the Human EEG. Computational and Mathematical Methods in Medicine, 2013.
39. Phneah, S.W. and Nisar, H., EEG-based alpha neurofeedback training for mood enhancement. Australasian Physical & Engineering Sciences in Medicine, 2017. 40(2): p. 325-336.
40. Qin, Y., Xu, P. and Yao, D., A comparative study of different references for EEG default mode network: The use of the infinity reference. Clinical Neurophysiology, 2010. 121(12): p. 1981-1991.
41. Bagby, R.M., Ryder, A.G., Schuller, D.R., et al., The Hamilton depression rating scale: Has the gold standard become a lead weight? American Journal of Psychiatry, 2004. 161(12): p. 2163-2177.
42. Hao, A., Huang, J. and Xu, X., Anxiety and depression in glioma patients: prevalence, risk factors, and their correlation with survival. Irish Journal of Medical Science, 2021. 190(3): p. 1155-1164.
43. Markou, A., Kosten, T.R. and Koob, G.F., Neurobiological similarities in depression and drug dependence: A self-medication hypothesis. Neuropsychopharmacology, 1998. 18(3): p. 135-174.
44. Yao, D.Z., A method to standardize a reference of scalp EEG recordings to a point at infinity. Physiological Measurement, 2001. 22(4): p. 693-711.
45. Jefferys, J.G.R., Traub, R.D. and Whittington, M.A., Neuronal networks for induced '40 Hz' rhythms. Trends in Neurosciences, 1996. 19(5): p. 202-208.
46. Yiou, P., Baert, E. and Loutre, M.F., Spectral analysis of climate data. Surveys in Geophysics, 1996. 17(6): p. 619-663.
47. He, Y. and Evans, A., Graph theoretical modeling of brain connectivity. Current Opinion in Neurology, 2010. 23(4): p. 341-350.
48. Rubinov, M. and Sporns, O., Complex network measures of brain connectivity: Uses and interpretations. Neuroimage, 2010. 52(3): p. 1059-1069.
49. Blankertz, B., Tomioka, R., Lemm, S., et al., Optimizing spatial filters for robust EEG single-trial analysis. Ieee Signal Processing Magazine, 2008. 25(1): p. 41-56.
50. Smola, A.J. and Scholkopf, B., A tutorial on support vector regression. Statistics and Computing, 2004. 14(3): p. 199-222.

51. Lin, S.-W., Ying, K.-C., Chen, S.-C., et al., Particle swarm optimization for parameter determination and feature selection of support vector machines. Expert Systems with Applications, 2008. 35(4): p. 1817-1824.
52. Zecca, L., Youdim, M.B.H., Riederer, P., et al., Iron, brain ageing and neurodegenerative disorders. Nature Reviews Neuroscience, 2004. 5(11): p. 863-873.
53. Elvevag, B. and Goldberg, T.E., Cognitive impairment in schizophrenia is the core of the disorder. Critical Reviews in Neurobiology, 2000. 14(1): p. 1-21.
54. Koles, Z.J., THE QUANTITATIVE EXTRACTION AND TOPOGRAPHIC MAPPING OF THE ABNORMAL COMPONENTS IN THE CLINICAL EEG. Electroencephalography and Clinical Neurophysiology, 1991. 79(6): p. 440-447.
55. Naeem, M., Brunner, C. and Pfurtscheller, G., Dimensionality reduction and channel selection of motor imagery electroencephalographic data. Computational intelligence and neuroscience, 2009: p. 537504-537504.
56. Pearson, J.M., Hickey, P.T., Lad, S.P., et al., Local Fields in Human Subthalamic Nucleus Track the Lead-up to Impulsive Choices. Frontiers in Neuroscience, 2017. 11.
57. Arnts, H., van Erp, W.S., Boon, L.I., et al., Awakening after a sleeping pill: Restoring functional brain networks after severe brain injury. Cortex, 2020. 132: p. 135-146.
58. Nakajima, K., Takahashi, M., Oishi, S., et al., Relationship between psychiatric symptoms and regional cerebral blood flow in patients with mild Alzheimer's disease. Psychogeriatrics, 2008. 8(3): p. 108-113.
59. Moller, E., Schack, B., Arnold, M., et al., Instantaneous multivariate EEG coherence analysis by means of adaptive high-dimensional autoregressive models. Journal of Neuroscience Methods, 2001. 105(2): p. 143-158.
60. Hesse, W., Moller, E., Arnold, M., et al., The use of time-variant EEG Granger causality for inspecting directed interdependencies of neural assemblies. Journal of Neuroscience Methods, 2003. 124(1): p. 27-44.
61. Chikara, R.K., Ko, L.-W. and Ieee. Classification of EEG-P300 Signals Using Phase Locking Value and Pattern Recognition Classifiers. in Conference on Technologies and Applications of Artificial Intelligence (TAAI). 2015. Tainan, TAIWAN.

Tables

Table I. The accuracy of the differentiation between E-AD patients and E-no-AD patients based on the network property, principal component, and SPN features of functional networks in different frequency bands.

Evaluation metrics	Frequency band	Network property	PCA	SPN
ACC	Delta	58.91±1.24%	64.01±0.62%	73.72±1.12%
	Theta	59.02±0.76%	61.83±0.45%	84.37±0.96%
	Alpha	60.12±0.68%	67.08±0.53%	81.62±0.89%
	Beta	62.05±0.62%	68.97±0.45%	89.90±0.69%
	Gamma	58.97±0.85%	64.38±0.53%	81.74±1.32%
	Full frequency	58.97±0.96%	65.50±0.33%	85.95±1.26%
SEN	Delta	28.50±1.18%	32.07±1.09%	64.54±1.73%
	Theta	30.80±0.89%	25.24±0.66%	81.69±1.61%
	Alpha	32.61±0.82%	36.68±0.64%	76.36±1.02%
	Beta	33.40±1.20%	36.83±0.82%	87.37±0.96%
	Gamma	30.89±1.12%	22.85±0.59%	74.19±1.10%
	Full frequency	29.98±0.86%	24.29±0.64%	82.48±0.93%
SPE	Delta	80.07±0.95%	86.24±1.30%	80.11±1.18%
	Theta	78.66±1.28%	87.28±0.82%	86.24±0.71%
	Alpha	79.26±0.76%	88.23±0.64%	85.28±1.02%
	Beta	80.84±0.39%	91.33±0.76%	91.67±0.78%
	Gamma	78.50±1.02%	93.27±0.64%	87.00±1.78%
	Full frequency	79.13±0.94%	94.18±0.50%	88.37±2.04%

Figures

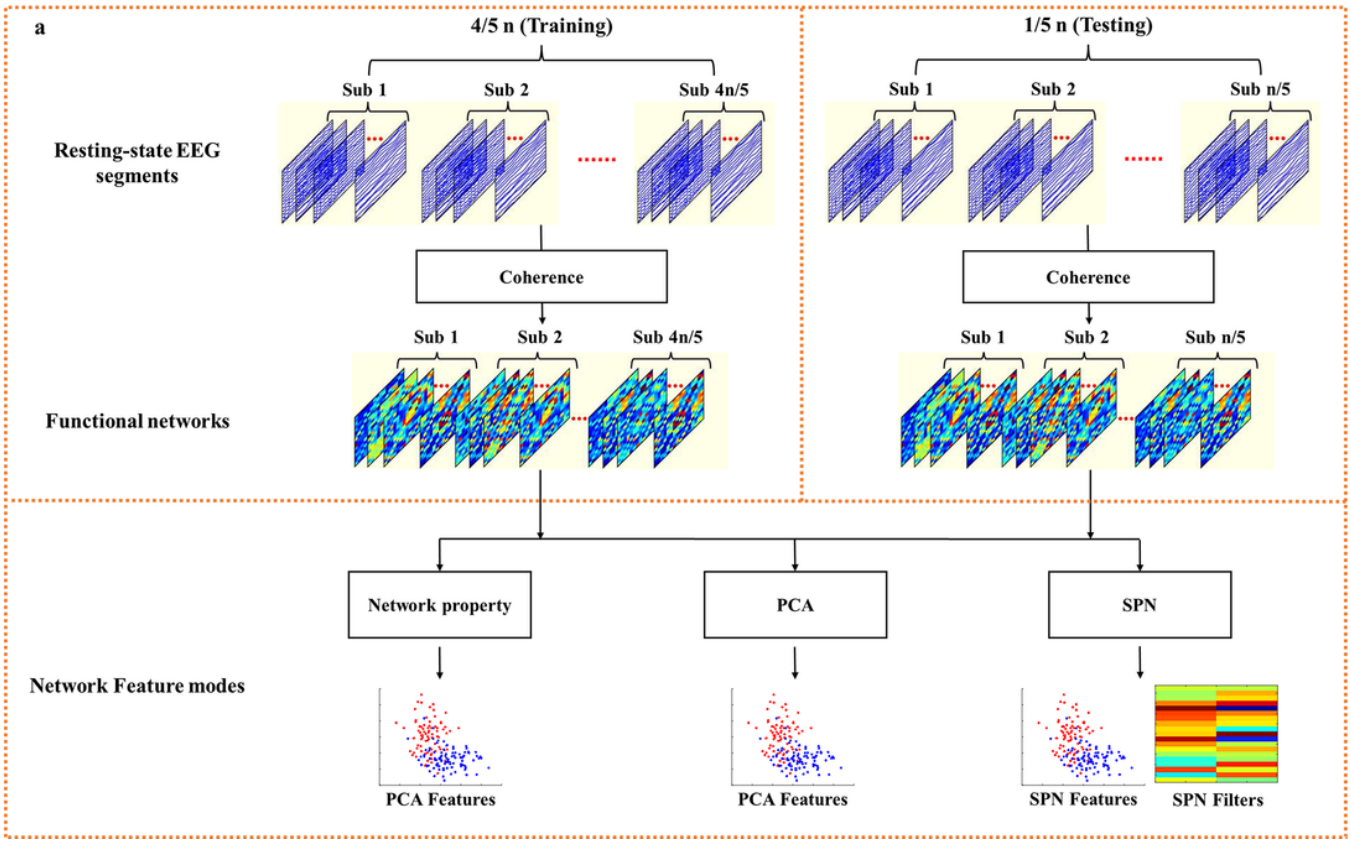

Figure 1

The procedures of differentiating between E-AD patients and E-no-AD patients based on resting-state EEG segments. (a) The process of constructing the functional networks from the training dataset. (b) Building the functional networks from the testing dataset. (c) Extracting the network features from the functional networks for the differentiation of E-AD patients and E-no-AD patients.

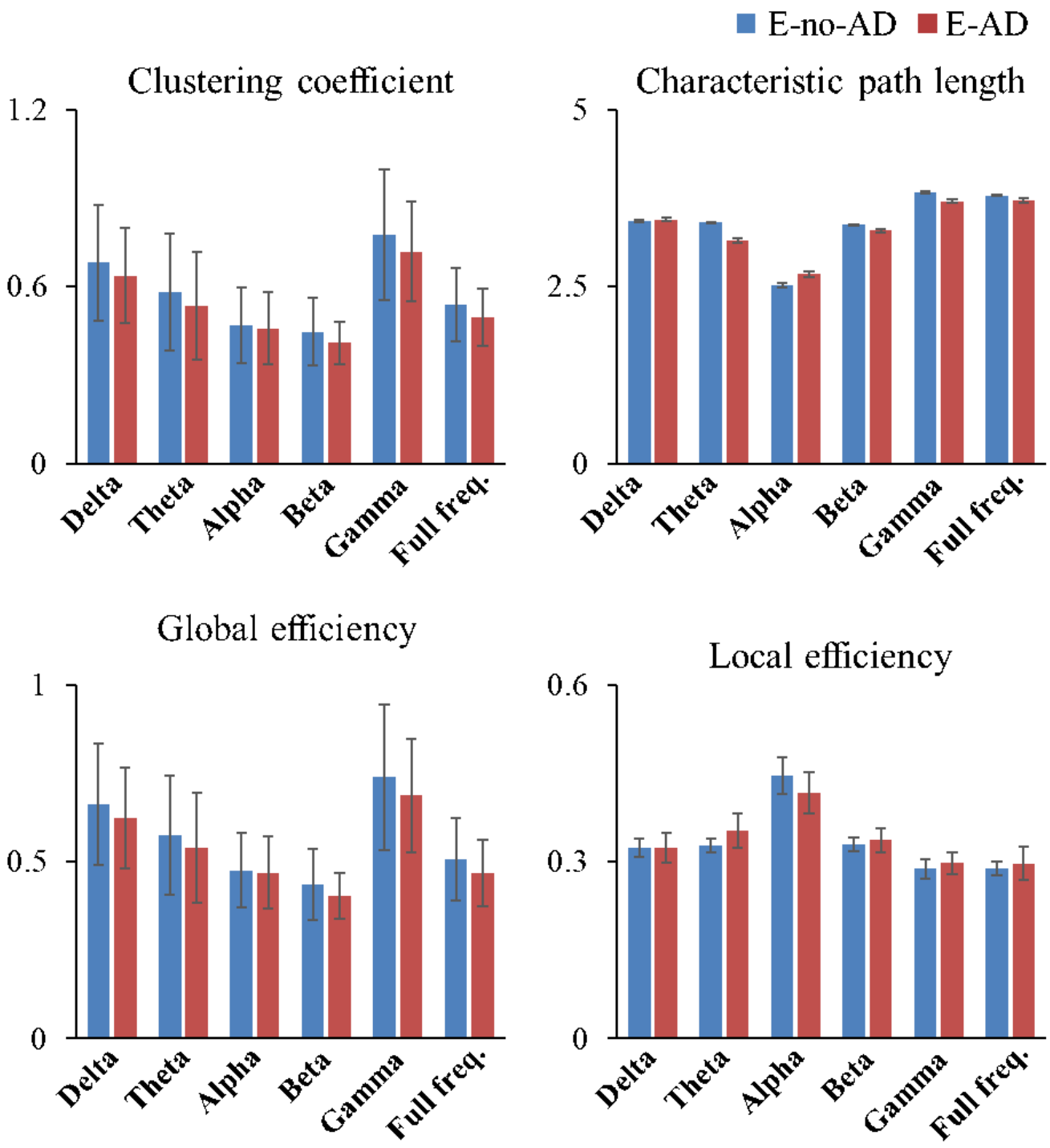

Figure 2

Four network properties of functional networks in different frequency bands for E-AD patients and E-no-AD patients. (Delta: 0.1–4 Hz, Theta: 4–8 Hz, Alpha: 8–13 Hz, Beta: 13–30 Hz, Gamma: 30–100 Hz, and full-frequency band: 0.1–100 Hz).

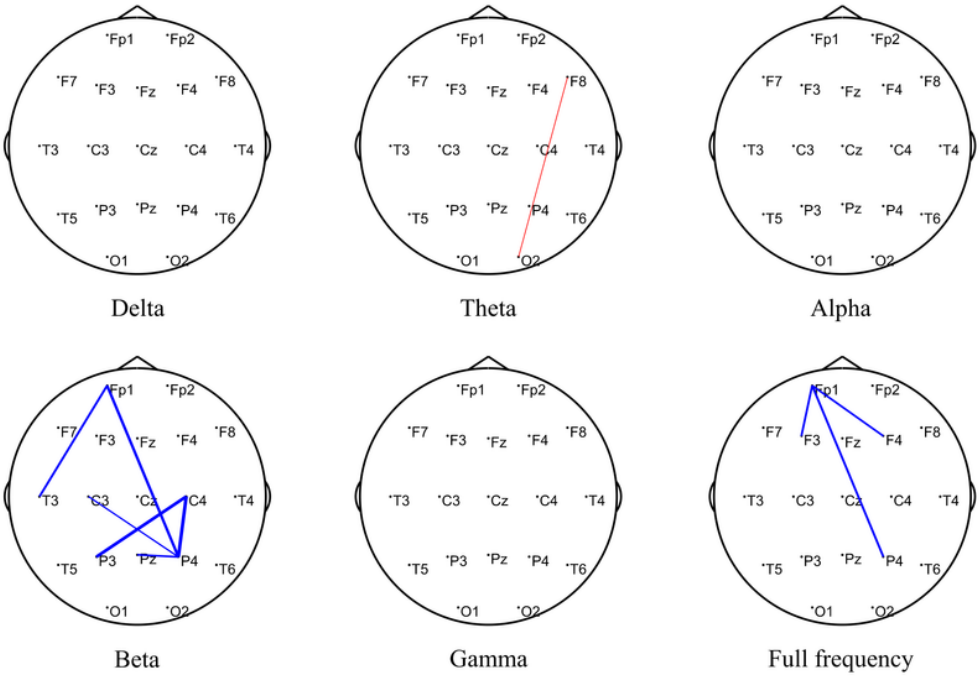

Figure 3

The statistical comparison of the functional networks in different frequency bands. The red/blue lines representing the corresponding connection strength of E-AD patients is significantly stronger/weaker than for E-no-AD patients.

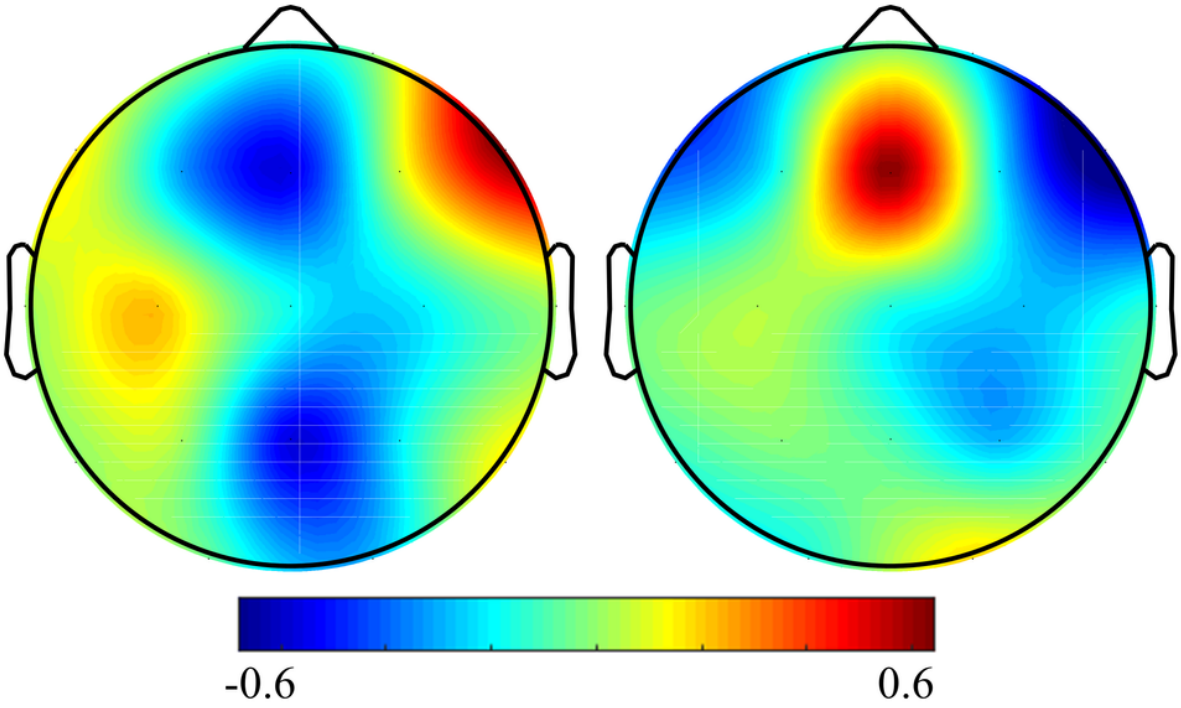

Figure 4

The scalp topologies for the first pairs of SPN filters extracted from beta-band functional networks with the best classification performance. The red/blue areas represent the critical brain regions with stronger/weaker connectivity strengths in the functional networks.